

# Kinetic Laws of the Reaction of Dimethyl Ether Synthesis from Synthesis-Gas

Jasur Shukurov<sup>1,\*</sup>, Normurot Fayzullaev<sup>2</sup>

<sup>1</sup>Doctoral student of Samarkand State University, Samarkand, Uzbekistan

<sup>2</sup>Doctor of Technical Sciences, Professor, Department of Polymer Chemistry and Chemical Technology, Samarkand State University, Samarkand, Republic of Uzbekistan

**Abstract** In the article, more than 20 catalysts were tested for synthesis gas dimethyl ether. Among them, catalysts containing  $\text{Al}_2\text{O}_3 \cdot \text{CuO} \cdot \text{ZnO} \cdot \text{ZrO}_2 / \text{HSZ}$  and  $\text{Cr}_2\text{O}_3 \cdot \text{Al}_2\text{O}_3 \cdot \text{ZnO} / \text{HSZ}$  were proven to have high catalytic activity and productivity. In the presence of these catalysts, it was found that during the reaction, coke and tars are formed in minimal amount, and the catalyst works without changing its catalytic activity for a long time. Therefore,  $\text{Al}_2\text{O}_3 \cdot \text{CuO} \cdot \text{ZnO} \cdot \text{ZrO}_2 / \text{HSZ}$  and  $\text{Cr}_2\text{O}_3 \cdot \text{Al}_2\text{O}_3 \cdot \text{ZnO} / \text{HSZ}$  catalysts with the following composition were used for methanol synthesis. Two-flow devices were used to conduct catalytic experiments: 2-4 MPa in the pressure range and 0.2-0.6 MPa (low-pressure device) in the range. Catalyst activation was conducted in a nitrogen-hydrogen stream ( $\approx 2$  Vol.%  $\text{H}_2$  at  $\text{N}_2$ , consumption  $\approx 2$  l/h). Contact Time, s·kg<sub>cat</sub>/l defined by the formula:  $\tau = 3600m/V_{\text{kir}}$ , conversion of methanol to dimethyl ether (DME) calculated by the formula:  $X_{\text{CH}_3\text{OH}} = 2C_{\text{DME}} \cdot 100(2C_{\text{DME}} + C_M)$ . The conversion of methanol to DME rises as contact duration increases (volumetric velocity decreases). Pressure reduction reduces the rate of methanol production but does not affect methanol dehydration. As a result, the higher the methanol synthesis, the lower the pressure at the same contact time.

**Keywords** Synthesis-gas, Methanol, Dimethyl ether, Volumetric rate, Temperature

## 1. Introduction

One of the most important processes in the chemical industry is the deep processing of natural gas, petroleum satellite gas, biogas, and others into valuable petrochemical products [1,2], and the conversion of natural and petroleum satellite gas into easily transportable products allows natural resources to be transferred to universal energy reserves [3-7]. In the years since scientists all around the world have been fascinated by the process of converting synthesis gas into dimethyl ether at one stage.

The composition and properties of the ethylene series hydrocarbons obtained from dimethyl ether are determined by the physicochemical properties of the zeolite catalyst used in this process, texture characteristics, extraction methods and conditions, and the ratio of gas and hydrogen in the synthesis-gas composition. Controlling the acidic properties of high-silicon zeolites as well as the initial synthesis-gas composition allows for the production of a light sulfur-free synthetic oil from methanol and dimethyl ether [8-10]. The acidic properties of zeolites are known to

be dependent on the nature of the exchange cations [11-13] and the technique of their introduction [14-16]. Nowadays, in commercial synthesis via methanol-in getting hydrocarbons such as ethylene, propylene, and butylenes from gas, ZSM-5 type catalysts [17] and Sapo-34 type molecular sieves are frequently utilized as catalysts [18]. It is known that the synthesis of hydrocarbons such as ethylene, propylene and butylenes from dimethyl ether is easier than the synthesis of hydrocarbons such as ethylene, propylene and butylenes from methanol [16-23], which is why dimethyl ether is a stronger methylating agent compared to methanol [8-13], which allows the reaction of the synthesis of unsaturated hydrocarbons from dimethyl ether to be conducted with a sufficiently large. Furthermore, dimethyl ether has less activity than methanol in the hydrogen displacement processes that result in the formation of Coke, resulting in a reaction to obtain unsaturated hydrocarbons from dimethyl ether with a significantly lower rate of catalyst deactivation than the reaction with methanol. Currently, it is critical to generate organic synthesis and petrochemical products based on methane and acetylene-based syntheses. It is mostly used to oxy-conduct methane, aromatize methane and propane-butane fractions, synthesize methanol and dimethyl ether from methane and synthesis gas, and produce lower

\* Corresponding author:

abdulatif20131@gmail.com (Jasur Shukurov)

Received: Apr. 13, 2023; Accepted: Apr. 28, 2023; Published: May 12, 2023

Published online at <http://journal.sapub.org/ijmc>

molecular olefins from them. In these reactions, high-silicon zeolites are used as catalysts and trapping agents [25-41].

## 2. Experimental Part

For methanol synthesis, the following catalysts were used:  $\text{Al}_2\text{O}_3 \cdot \text{CuO} \cdot \text{ZnO} \cdot \text{ZrO}_2 / \text{HSZ}$  and  $\text{Cr}_2\text{O}_3 \cdot \text{Al}_2\text{O}_3 \cdot \text{ZnO} / \text{HSZ}$ . A chromatographic approach was used to evaluate the amount of chemicals at the reactor's outlet. Catalytic studies were carried out using two flow devices: 2-4 MPa in the pressure range and 0.2-0.6 MPa (low-pressure device) in the range. The reactor's inner diameter is 11 mm, while the thermocouple channel's outer diameter is 4 mm. The catalyst torque was 0.5 g mass, with a fraction of 0.25-0.315 mm. The temperature of the catalytic floor is measured using two stainless steel thermocouples (wall thickness 0.25 mm) (the diameter of the thermocouple at the entrance and exit from the floor is 1 mm). A Porapak T colon is used to determine DME, methanol, and water. Catalyst activation was carried out in a nitrogen-hydrogen current (2 Vol.%  $\text{H}_2$  at  $\text{N}_2$ , consumption 2 l/h). When conducting catalytic tests, synthesis is performed-gas composition and volume %:  $\text{CO}$ -21,8;  $\text{CO}_2$ -5,2;  $\text{N}_2$ -5,3;  $\text{H}_2$ -67,7.

Contact time,  $\tau \cdot \text{kg}_{\text{cat}}/\text{l}$ , determined by the formula:

$$\tau = 3600m / V_{kir}$$

Where  $m$  is the tensile mass, kg; - load on raw materials brought to normal conditions, l/h.

The conversion of methanol to DME was calculated using the formula:

$$X_{\text{CH}_3\text{OH}} = 2C_{\text{DME}} \cdot 100(2C_{\text{DME}} + C_{\text{M}}),$$

Here  $C_{\text{DME}}$ ,  $C_{\text{M}}$ - volumetric concentrations of DME and methanol at the exit of the reactor, respectively.

X-ray phase analysis (XPA) of the samples was performed on a Shimadzu XRD-7000 diffractometer in  $\text{CuK}_\alpha$  radiation ( $\lambda = 1.5418 \text{ \AA}$ ). The morphology of the samples was studied using a JEOL JSM 6390 LA scanning electron microscope (SEM) (Japan).

## 3. Results and Discussion

Compositions including methanol (methanol synthesis catalyst) and dehydrating (methanol dehydration catalyst) components are commonly utilized in the direct synthesis of DME. At 2-4 MPa and 260-320°C, the kinetics of direct synthesis of DME from synthesis gas were investigated in bifunctional catalysts including  $\text{Al}_2\text{O}_3 \cdot \text{CuO} \cdot \text{ZnO} \cdot \text{ZrO}_2 / \text{HSZ}$  and  $\text{Cr}_2\text{O}_3 \cdot \text{Al}_2\text{O}_3 \cdot \text{ZnO} / \text{HSZ}$ . The volume decreases during the synthesis of dimethyl ether from gas and hydrogen, thus the process was carried out at high temperatures; the influence of temperature on the yield of dimethyl ether is illustrated in Figure 1. It can be seen that the conversion of carbon dioxide increases with increasing

pressure, with the production of dimethyl ether having the greatest value at a pressure of 1 MPa (Fig. 1).

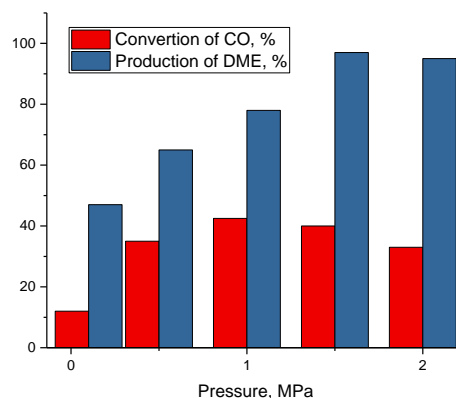


**Figure 1.** Effect of pressure on CO gas conversion and dimethyl ether yield ( $T=300^\circ\text{C}$ , hydrogen: Carbon monoxide=2, volumetric rate 1000  $\text{hour}^{-1}$ .)

The decrease in the yield of dimethyl ether can be explained by its decomposition

$\text{CH}_3\text{OCH}_3 \leftrightarrow \text{CH}_4 + \text{CO} + \text{H}_2$ . As the temperature increases, soot gas conversion and dimethyl ether yield increase (Figure 2).

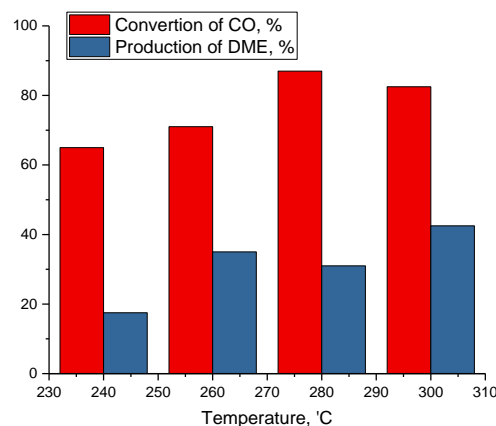


**Figure 2.** Effect of temperature on carbon monoxide conversion and dimethyl ether yield ( $T=300^\circ\text{C}$ , hydrogen: Carbon monoxide=2, volumetric rate 1000  $\text{hour}^{-1}$ .)

As shown in Fig. 3, as volume velocity increases, the conversion of CO gas and the production of dimethyl ether decrease (Fig. 3). The reason for this is that the contact time of the reagents with the catalyst surface decreases with increasing volumetric rate, reducing gas conversion because the interaction between the reagents and the catalyst surface does not have time to occur in the gas phase due to the low contact time. At the same time, an increase in the mole ratio of carbon dioxide and hydrogen leads to an increase in the yield of dimethyl ether and the conversion of carbon dioxide (Fig. 3).

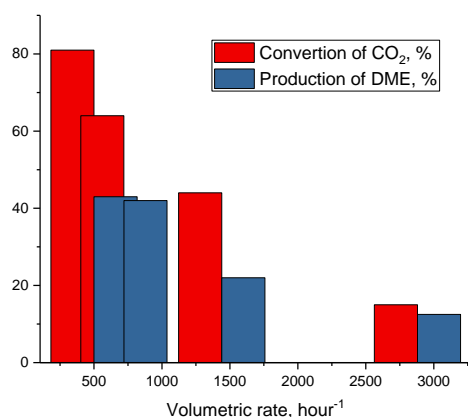


**Figure 3.** Effect of volumetric rate on the conversion of Carbon monoxide gas and dimethyl ether yield P=1 MPa, T=300°C, hydrogen: Carbon monoxide, volumetric rate 1000 hour<sup>-1</sup>

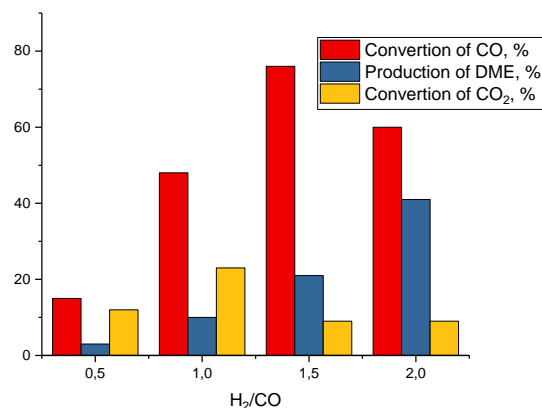


**Figure 4.** Effect of hydrogen: carbon monoxide molar ratio on the conversion of nitrous oxide and dimethyl ether volume and carbon dioxide concentration (T=300°C, P=1 MPa, volumetric rate 1000 hour<sup>-1</sup>.)

According to studies on the influence of the key parameters on the efficiency of the process of dimethyl ether extraction from synthesis gas, raising the pressure, temperature, and hydrogen: hot gas mole ratio leads to an increase in dimethyl ether yield and hot gas conversion. As a result, the following ideal conditions for generating dimethyl ether from hydrogen gas in a single step were determined:

P=1 MPa, T=300°C, hydrogen: carbon monoxide = 2, volumetric rate 1000 h<sup>-1</sup>. In this case, the conversion of Carbon monoxide does not decrease for 220 hours. Figure 2 shows data on the activation of bifunctional catalysts manufactured in a high-pressure device. H<sub>2</sub>-absorption and water formation are observed during heating, beginning at 160°C. As a result, the greatest water separation peak coincides with the minimum hydrogen concentration at the reactor's exit (Fig. 5).

Since the chosen temperature range allows for a sufficiently "soft" reduction of the catalyst, increasing the temperature to 200°C results in a small additional reduction

of the catalyst, as seen by weak peaks of H<sub>2</sub> absorption and water separation (between 600-700 min).

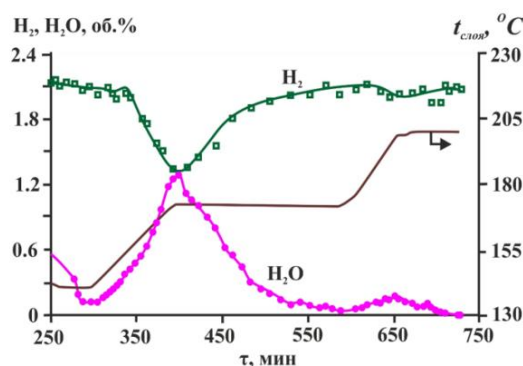


**Figure 5.** Al<sub>2</sub>O<sub>3</sub>\*CuO\*ZnO\*ZrO<sub>2</sub>/HSZ and Cr<sub>2</sub>O<sub>3</sub>\*Al<sub>2</sub>O<sub>3</sub>\*ZnO/HSZ catalysts (1:1)

The minor increase in water evolution over the corresponding hydrogen absorption observed up to about 500 min in the reduction is due to the dehydroxylation of the oxide present in the bifunctional catalyst, as demonstrated by studies using the original alumina.

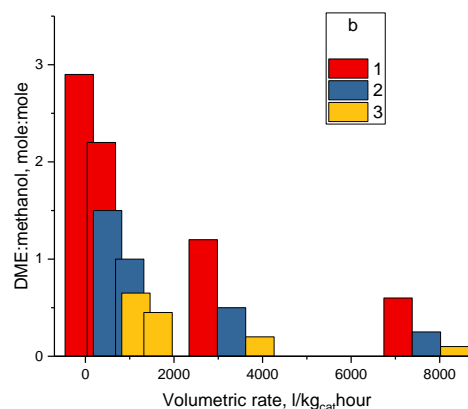
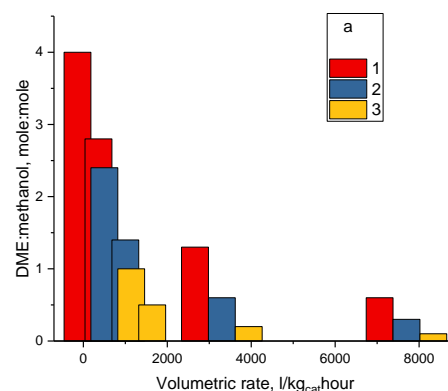


**Figure 6.** DME: methanol mole ratio dependence on the volumetric rate. MPa pressure: a - 2; b - 4. Temperatures in degrees Celsius: 1 -320; 2 -300; 3 -280

Figure 6a-6b shows the findings of a study on the effect of

volume velocity, temperature, and pressure on the DME: methanol ratio.

The temperature-programmed return spectrum of the  $\text{Al}_2\text{O}_3*\text{CuO}*\text{ZnO}*\text{ZrO}_2/\text{HSZ}$  catalyst is shown in Figure 7. The temperature is derived from programmed return data, which indicates that the commencement of the copper oxide return is around 165°C.

The total hydrogen absorption is quantitatively consistent with the return of copper oxide from the catalyst.

The investigation of the textural properties of the catalysts showed that when treated in hydrogen or helium flow, the specific surface area of the  $\text{Al}_2\text{O}_3*\text{CuO}*\text{ZnO}*\text{ZrO}_2/\text{HSZ}$  catalyst decreases from 138 to 82 m<sup>2</sup>/g and the average diameter of the pores increases from 13 to 21 nm.

Micrographs of the  $\text{Al}_2\text{O}_3*\text{CuO}*\text{ZnO}*\text{ZrO}_2/\text{HSZ}$  catalyst used for methanol production under various processing conditions are shown in Figure 7. The initial

$\text{Al}_2\text{O}_3*\text{CuO}*\text{ZnO}*\text{ZrO}_2/\text{HSZ}$  catalyst surface (Fig. 8a) is inhomogeneous, rough, and covered with individual particles.

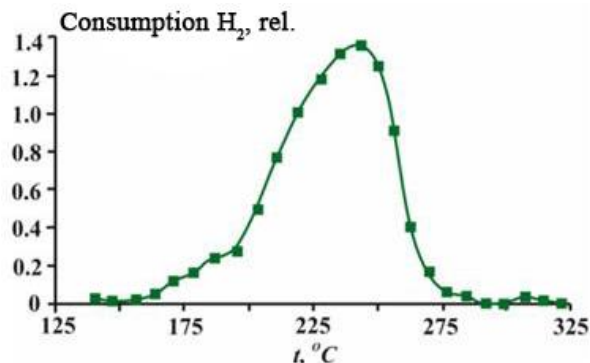
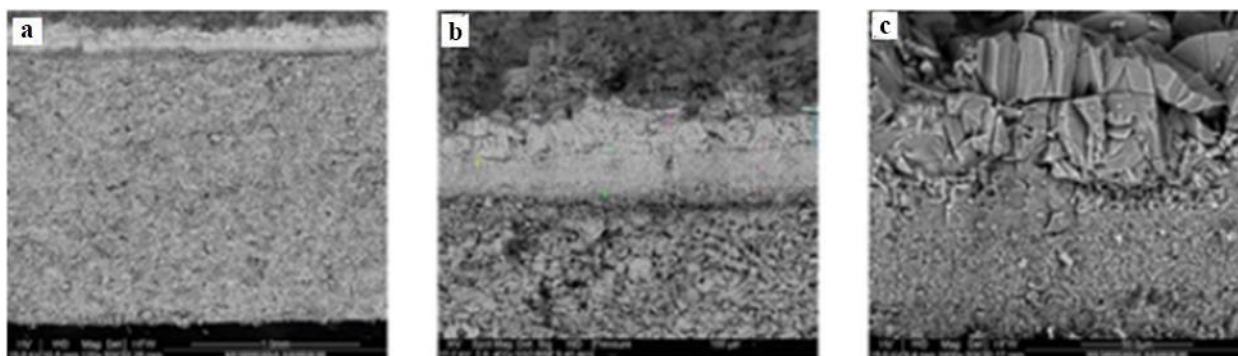


**Figure 7.** Temperature programmed reduction spectrum of  $\text{CuO}*\text{ZnO}*\text{Al}_2\text{O}_3*\text{ZrO}_2/\text{HSZ}$  catalyst



a - initial, b - treated with hydrogen at 320°C for 4 hours, c - after being used in synthesis in the presence of hydrogen: is gas for 70 hours at  $T=200-300^\circ\text{C}$ , ( $P=1-5$  MPa).

**Figure 8.** Micrographs of  $\text{Al}_2\text{O}_3*\text{CuO}*\text{ZnO}*\text{ZrO}_2/\text{HSZ}$  sample

SEM images of the catalysts are depicted in Figure 8. Treated with hydrogen at 320°C for 4 hours, the catalyst brand consists of particles forming aggregates of a loose sponge-like structure. After being used in synthesis in the presence of hydrogen, the catalyst is a "monolithic" structure consisting of aggregates of various sizes and shapes.

Reduction in hydrogen leads to the high porosity of the surface and the formation of individual particles. After testing the catalyst in the synthesis of carbon dioxide and hydrogen dimethyl ether, when the temperature was changed from 200 to 300°C and the pressure was changed in the range of 1-2 MPa, the textural characteristics of the catalyst changed significantly (Fig. 8c), that is, the surface became smoother, the average size of the pores changed from 1 to 40 μm.

The heating rate with air flow is 10°C/min even though the catalyst worked for more than 120 hours, no change in its surface was expected, that is, the carbon layer was almost not formed on the surface (Fig. 9). Figure 9 shows that two effects are observed in the derivativeograms. The first exo-effect with a temperature of 192°C also consists of two effects.

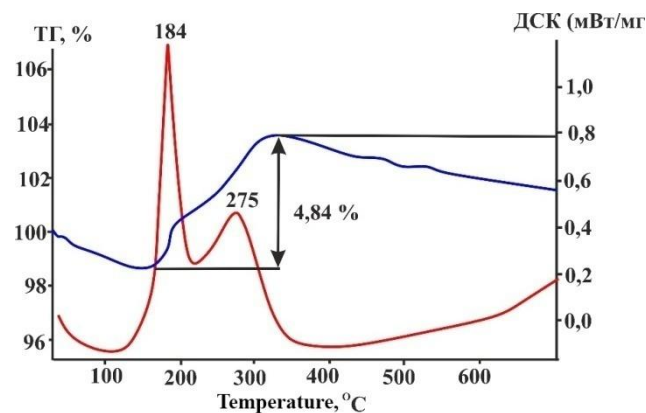


**Figure 9.** Differential thermal analysis of treated catalyst sample after 70 hours of use

The first is the release of carbon dioxide from the catalyst surface as a result of carbon combustion, which was confirmed by differential thermal analysis data and the temperature-controlled oxidation method. The second peak is observed at 275°C, indicating that the total mass gain is 4.84%.

## 4. Conclusions

The conversion of methanol to DME increases as the contact time grows (volumetric rate lowers), approaching the thermodynamic equilibrium value. A decrease in pressure reduces the rate of methanol production but has no effect on methanol dehydration. As a result, the higher the methanol synthesis, the lower the pressure at the same contact time. The presence of methanol in the reaction products is caused by the thermodynamics of the dehydration reaction. The DME: methanol ratio can be changed by changing the direct synthesis conditions.

## REFERENCES

- [1] Gentzen, M., Doronkin, D.E., Sheppard, T.L., Grunwaldt, J.D., Sauer, J. and Behrens, S., 2018. An intermetallic Pd2Ga nanoparticle catalyst for the single-step conversion of CO-rich synthesis gas to dimethyl ether. *Applied Catalysis A: General*, 562, pp.206-214.
- [2] Арутюнов, В.С., 2008. Мировая газохимия сегодня (Итоги 8-го Международного симпозиума по конверсии природного газа-NGCSVIII). *Катализ в промышленности*, (1), pp.51-58.
- [3] Simonetti, D.A., Carr, R.T. and Iglesia, E., 2012. Acid strength and solvation effects on methylation, hydride transfer, and isomerization rates during catalytic homologation of C1 species. *Journal of catalysis*, 285(1), pp.19-30.
- [4] Matieva, Z.M., Kurumov, S.A., Snatenkova, Y.M., Kolesnichenko, N.V., Bondarenko, G.N. and Khadzhiev, S.N., 2019. Conversion of Dimethyl Ether to a Mixture of Liquid Hydrocarbons with Increased Triptane Content. *Russian Journal of Applied Chemistry*, 92, pp.235-243.
- [5] Ahn, J.H., Temel, B. and Iglesia, E., 2009. Selective homologation routes to 2, 2, 3-trimethylbutane on solid acids. *Angewandte Chemie International Edition*, 48(21), pp.3814-3816.
- [6] Simonetti, D.A., Ahn, J.H. and Iglesia, E., 2011. Mechanistic details of acid-catalyzed reactions and their role in the selective synthesis of triptans and isobutane from dimethyl ether. *Journal of Catalysis*, 277(2), pp.173-195.
- [7] Otalvaro, N.D., Kaiser, M., Delgado, K.H., Wild, S., Sauer, J. and Freund, H., 2020. Optimization of the direct synthesis of dimethyl ether from CO<sub>2</sub> rich synthesis gas: closing the loop between experimental investigations and model-based reactor design. *Reaction Chemistry & Engineering*, 5(5), pp.949-960.
- [8] Khadzhiev, S.N., Kolesnichenko, N.V., Markova, N.A., Bukina, Z.M., Ionin, D.A. and Kulumbegov, R.V., 2012. RU Patent No. 2442650.
- [9] Bukina Z.M., Grafova G.M., Ionin D.A., Kolesnichenko N.V., Lin G.I., Markova N.A., Khadzhiev S.N. Patent PF No. 2442767. 2012.
- [10] Patent RF No. 2616981. 2017.
- [11] Stiefel, M., Ahmad, R., Arnold, U. and Döring, M., 2011. Direct synthesis of dimethyl ether from carbon-monoxide-rich synthesis gas: Influence of dehydration catalysts and operating conditions. *Fuel Processing Technology*, 92(8), pp.1466-1474.
- [12] Lee, K.Y., Lee, S.W. and Ihm, S.K., 2014. Acid strength control in MFI zeolite for the methanol-to-hydrocarbons (MTH) reaction. *Industrial & Engineering Chemistry Research*, 53(24), pp.10072-10079.
- [13] Ratamanalaya, P., Limtrakul, S., Vatanatham, T. and Ramachandran, P.A., 2011. Kinetics Study of Direct Dimethyl Ether Synthesis. In *TICHe International Conference*. Hatyai.
- [14] Song, J.W., Lam, S.M., Fan, X., Cao, W.J., Wang, S.Y., Tian, H., Chua, G.H., Zhang, C., Meng, F.P., Xu, Z. and Fu, J.L., 2020. Omics-driven systems interrogation of metabolic dysregulation in COVID-19 pathogenesis. *Cell metabolism*, 32(2), pp.188-202.
- [15] Björger, M., Joensen, F., Holm, M.S., Olsbye, U., Lillerud, K.P. and Svelle, S., 2008. Methanol to gasoline over zeolite H-ZSM-5: Improved catalyst performance by treatment with NaOH. *Applied Catalysis A: General*, 345(1), pp.43-50.
- [16] Rac, V., Rakić, V., Miladinović, Z., Stošić, D. and Auroux, A., 2013. Influence of the desilication process on the acidity of HZSM-5 zeolite. *Thermochimica Acta*, 567, pp.73-78.
- [17] Van Der Bij, H.E., Aramburo, L.R., Arstad, B., Dynes, J.J., Wang, J. and Weckhuysen, B.M., 2014. Phosphatation of Zeolite H-ZSM-5: A Combined Microscopy and Spectroscopy Study. *ChemPhysChem*, 15(2), pp.283-292.
- [18] Rahmani, F., Haghighi, M. and Estifae, P., 2014. Synthesis and characterization of Pt/Al<sub>2</sub>O<sub>3</sub>-CeO<sub>2</sub> nanocatalyst used for toluene abatement from waste gas streams at low temperature: Conventional vs. plasma-ultrasound hybrid synthesis methods. *Microporous and Mesoporous Materials*, 185, pp.213-223.
- [19] Zaidi, H.A. and Pant, K.K., 2014. An oxalic-acid-treated ZnO/CuO/HZSM-5 catalyst with high resistance to coke formation for the conversion of methanol to hydrocarbons. *International Journal of Green Energy*, 11(4), pp.376-388.
- [20] Ibodullayevich, F.N., Yunusovna, B.S. and Anvarovna, X.D., 2020. Physico-chemical and texture characteristics of Zn-Zr/VKTS catalyst. *Journal of Critical Reviews*, 7(7), pp.917-920.
- [21] Mamadoliev, I.I., Khalikov, K.M. and Fayzullaev, N.I., 2020. Synthesis of high silicon zeolites and their sorption properties. *International Journal of Control and Automation*, 13(2), pp.703-709.
- [22] Mamadoliev, I.I. and Fayzullaev, N.I., 2020. Optimization of the activation conditions of high silicon zeolite. *International Journal of Advanced Science and Technology*, 29(3), pp.6807-6813.
- [23] Temirov, F.N., Khamroyev, J.K., Fayzullayev, N.I., Haydarov, G.S. and Jalilov, M.K., 2021, September. Hydrothermal synthesis of zeolite HSZ-30 based on kaolin. In *IOP Conference Series: Earth and Environmental Science* (Vol. 839, No. 4, p. 042099). IOP Publishing.
- [24] Park, H.W., Ha, J.K. and Lee, E.S., 2014. Kinetic mechanism of dimethyl ether production process using syngas from integrated gasification combined cycle power plant. *Korean*

- Journal of Chemical Engineering*, 31, pp.2130-2135.
- [25] Buronov, F. and Fayzullayev, N., 2022, June. Synthesis and application of high silicon zeolites from natural sources. In *AIP Conference Proceedings* (Vol. 2432, No. 1, p. 050004). AIP Publishing LLC.
- [26] Tursunova, N.S. and Fayzullaev, N.I., 2020. Kinetics of the reaction of oxidative dimerization of methane. *International Journal of Control and Automation*, 13(2), pp.440-446.
- [27] Fayzullaev, N.I. and Fayzullaev, O.O., 2004. Kinetic regularities in the reaction of the oxidizing condensation of methane on applied oxide catalysts. *Khimicheskaya Promyshlennost*, 4, pp.204-207.
- [28] Muradov, K.M. and Fayzullaev, N.I., 2003. Technology for producing ethylene using the reaction of the oxidizing condensation of methane. *Khimicheskaya Promyshlennost*, 6, pp.3-7.
- [29] Sarimsakova, N.S., Atamirzayeva, S.T., Fayzullaev, N.I., Musulmonov, N.X. and Ibodullayeva, M.N., 2020. Kinetics and mechanism of reaction for producing ethyl acetate from acetic acid. *International Journal of Control and Automation*, 13(2), pp.373-382.
- [30] Omanov, B.S., Fayzullaev, N.I., Musulmonov, N.K., Xatamova, M.S. and Asrorov, D.A., 2020. Optimization of vinyl acetate synthesis process. *International Journal of Control and Automation*, 13(1), pp.231-238.
- [31] Omanov, B.S., Fayzullaev, N.I. and Xatamova, M.S., 2020. Vinyl acetate production technology. *International Journal of Advanced Science and Technology*, 29(3), pp.4923-4930.
- [32] Fayzullayev, N.I., Umirzakov, R.R. and Pardaeva, S.B., 2005. Study of acetylating reaction of acetylene by gas chromatographic method. In *ACS National Meeting Book of Abstracts* (pp. PETR-66).
- [33] Fayzullaev, N.I. and Muradov, K.M., 2004. Investigation of reaction of catalytic vapor-phase synthesis of vinyl acetate on applied catalyst. *Khimicheskaya Promyshlennost*, 3, pp.136-139.
- [34] Fayzullayev, N.I. and Umirzakov, R.R., 2005. To obtain acetone by spontaneous hydration of acetylene. In *ACS National Meeting Book of Abstracts* (pp. PETR-71).
- [35] Fayzullaev, N.I., Yusupov, D. and Shirinov, K., 2002. Sh.,... Keremetskaya, LV, Umirzakov, RR Catalytic vapor-phase hydration of acetylene and its derivatives. *Khimicheskaya Promyshlennost*, 7, pp.34-37.
- [36] Fayzullaev, N.I., 2004. Kinetics and mechanism of reaction of catalytic hydrochlorination of acetylene. *Khimicheskaya Promyshlennost*, 1, pp.49-52.
- [37] Aslanov, S.C., Buxorov, A.Q. and Fayzullayev, N.I., 2021. Catalytic synthesis of C<sub>2</sub>-C<sub>4</sub>-alkenes from dimethyl ether. *arXiv preprint arXiv:2104.03173*.
- [38] Bukhorov, A.Q., Aslanov, S.C. and Fayzullaev, N.I., 2022, June. Conversion of dimethyl ether to lower olefines. In *AIP Conference Proceedings* (Vol. 2432, No. 1, p. 050011). AIP Publishing LLC.
- [39] Bukhorov, A.Q., Aslanov, S.C. and Fayzullaev, N.I., 2022, June. Kinetic laws of dimethyl ether synthesis in synthesis gas. In *AIP Conference Proceedings* (Vol. 2432, No. 1, p. 050012). AIP Publishing LLC.
- [40] Khadzhiyev, S.N., Kolesnichenko, N.V., Khivrich, E.N. and Batova, T.I., 2019. Catalysts for Dimethyl Ether Conversion to Lower Olefins: Effect of Acidity, Postsynthesis Treatment, and Steam and Methanol Content in Feedstock. *Petroleum Chemistry*, 59, pp.427-437.
- [41] Musulmonov, N.X. and Fayzullaev, N.I., 2022, June. Textural characteristics of zinc acetate catalyst. In *AIP Conference Proceedings* (Vol. 2432, No. 1, p. 050015). AIP Publishing LLC.